International Journal of Mechanical Sciences 96-97 (2015) 101–109

Contents lists available at ScienceDirect

International Journal of Mechanical Sciences

journal homepage: www.elsevier.com/locate/ijmecsci

Non-linear energy harvesting from coupled impacting beams

K. Vijayan *, M.I. Friswell, H. Haddad Khodaparast, S. Adhikari

College of Engineering, Swansea University, Singleton Park, Swansea, SA2 8PP United Kingdom

ARTICLE INFO

Article history:
Received 4 October 2014
Received in revised form
26 January 2015
Accepted 5 March 2015
Available online 14 March 2015

Keywords:
Vibro-impact
Energy harvesting
Frequency-conversion
Piezoelectric
Modal reduction

ABSTRACT

Energy harvesting has many potential applications for structures with broadband excitation, such as aircraft noise and low frequency vibrations from human motion. The advantage with a vibro-impacting system is the capability of converting low frequency response to high frequencies. A coupled beam system is base excited and the influence of different system parameters are studied. Exciting the system at a single resonant frequency highlights the influence of clearance and base excitation amplitude on the beam responses. The frequency sweep study shows the sensitivity of the power generated to the contact stiffness, damping and clearance between the beams. The power generated by the coupled system from the non-linear impact is sensitive to the thickness ratio of the beams and the clearance. The variation in thickness ratio alters the spacing of the natural frequencies of the system which causes modes to interact. This study shows that higher power is produced than the linear system, depending on the dissimilarity in the mode shapes of the interacting close modes.

1. Introduction

The requirement for harvesting energy from low powered devices has gained impetus recently. Vibration-based MEMS energy harvesters have received increased attention as a potential power source for microelectronics and wireless sensor nodes. The purpose is to reduce or completely avoid battery replacement since these are generally placed at less accessible locations. These micro-systems are useful in built environment control, emergency response, monitoring and control of manufacturing processes and health monitoring of airframes, ships, cars and drilling [1].

There are different methods of transduction for vibration to electricity conversion such as piezoelectric, electromagnetic and electrostatic. These operate most effectively at frequencies more than 100 Hz [2–4]. Among the different transduction mechanisms piezoelectric transduction has received the most attention recently [5]. Typically piezoelectric harvesters consist of a cantilever beam with one or more piezoelectric patches mounted on a host vibrating structure.

Generally a low resonance frequency requires a large structure, and hence a major design challenge is to achieve small size and low resonant frequency. Limitations are imposed due to the micro-fabrication process and the brittle properties of silicon material. The power generated from the harvester is generally considered proportional to the cube of the excitation frequency and drops dramatically at low frequencies [6]. However there are a wide range of potential applications where it would be useful to harvest energy from low frequency vibration. The application areas range from human motion (<10 Hz), vehicle (<20 Hz) and machine vibrations (50 Hz) [7–9].

The principal challenge associated with these systems is the frequency range in which useful power can be extracted. Earlier studies of energy harvesting systems considered mostly linear stationary responses close to the resonance. This limitation is further aggravated by the fact that these micro-systems are also designed to have high quality factors to minimize the energy dissipation, further narrowing the optimal operating frequency band. Various techniques have been used to adjust the vibration characteristics of the harvester structure. These include attaching concentrated masses [10,11], varying the geometry of the structural member [12] and using mechanical preload for frequency adjustment [13]. However the above strategies are all still based on exciting the resonant frequency of a particular mode.

The effectiveness of linear oscillators reduces when the excitation from ambient vibration is distributed over a wide range of frequencies and when very low frequencies dominate the spectrum [7,14]. The requirement for an effective harvester in the low frequency range and for broadband excitation provided an impetus to exploit the effects of non-linearity. Various techniques have been explored to exploit the non-linearity, namely Duffing [15–18], impact [19–23] and bistable oscillator designs [24]. The present study will consider the non-linearity induced in the

* Corresponding author. Tel.: +44 1792 602969; fax: +44 1792 295676.
E-mail addresses: k.vijayan@swansea.ac.uk (K. Vijayan), m.i.friswell@swansea.ac.uk (M.I. Friswell), H.HaddadKhodaparast@swansea.ac.uk (H. Haddad Khodaparast), s.adhikari@swansea.ac.uk (S. Adhikari).

http://dx.doi.org/10.1016/j.ijmecsci.2015.03.001

system due to impact. Babitsky [25] analysed a vibro-impacting oscillator with symmetric stops and the effect of random vibration on the system. It was observed that the frequency of oscillation is high when the clearance is less than the standard deviation of the seismic mass displacement in the absence of stops. This finding has important implications from a design perspective to restrict the clearance.

Previous studies indicate that vibro-impact excites the higher modes of the system. The excitation of higher modes could result in higher power generation. For a linear system the harvester is usually designed to produce power at the resonant frequencies of the system. However with a non-linear vibro-impacting system, since the response becomes broadband, a robust harvester that is effective across a wide range of excitation frequencies could be designed. One of the configurations previously explored by various authors [26,27] to increase the number of resonant modes is the coupled structure. Yang et al. [26] analysed the effect on the energy harvested of a symmetric structure. The system consisted of two identical beams clamped at the base excitation end and the other end was attached to a concentrated mass by a spring element. However it has been found that asymmetry in the system can increase the response within the coupled linear system [28,29].

The present study will investigate the possibility of similar effects within a non-linear system. A system consisting of two beams with a localised non-linearity induced by an impact was modelled theoretically to explore the effect of frequency up conversion on the power generated from the harvester.

2. Model description

The schematic model of the system is shown in Fig. 1. The beams were clamped at one end and the whole system is base excited at frequency ω_e. A thickness ratio for the beams of 0.5 was chosen initially to analyse the influence of asymmetry on the system response. The dimensions of the system are given in Table 1, and the natural frequencies of the uncoupled system are given in Table 2. The displacements of the thin and the thick beams at the free ends are denoted by y_{1e} and y_{2e} respectively. The clearance between the beams is denoted by δ. The two beams behave independently without impact and during contact the beams motions are coupled through the non-linear contact. The system is excited both by the base excitation and by the non-linear impact.

A piecewise linear multi degree freedom system is considered for the analysis. Analytical formulation for the system is possible, however is not considered in the scope of the paper. The coupled system is modelled by finite element analysis using 30 Euler–Bernoulli elements for each beam. The impact force is given by

$$F_{\text{imp}} = K_{\text{cont}}((y_{2e}-y_{1e})-\delta) \quad \text{if} \quad y_{2e}-y_{1e} < \delta$$
$$= 0 \quad \text{Otherwise} \tag{1}$$

The contact element is active when the relative displacement $(y_{2e}-y_{1e})$ is less than the clearance (δ) between the beams. The non-linearity is induced by the intermittent contact occurring between the beams. The equation of motion of the whole system is

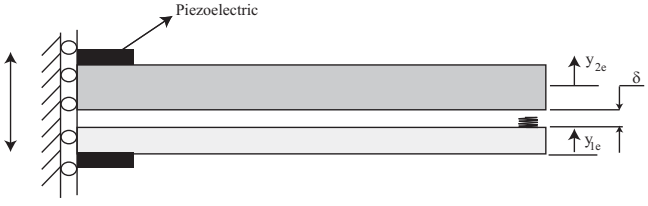

Fig. 1. Schematic of the energy harvester with the non-linearity induced from impact occurring at the tip.

Table 1
Dimensions of the coupled beam system.

Parameter	Value	Unit
Length of the beam	305	mm
Thickness of the beam 1	0.5	mm
Thickness of the beam 2	0.25	mm
Width of the beams	16	mm
Young's modulus	210	GPa
Mass of beam 1	140	g
Mass of beam 2	70	g
Density of beams	7000	kg/m^3

Table 2
Natural frequencies of the individual beams.

ω_{thin}(Hz)	ω_{thick}(Hz)
2.32	4.64
14.54	29.09
40.72	81.44
79.80	159.59

given by

$$\mathbf{M}\ddot{\mathbf{Y}}+\mathbf{C}\dot{\mathbf{Y}}+\mathbf{K}\mathbf{Y}+\mathbf{F}_{\text{imp}} = \alpha\mathbf{M}\{\mathbf{Y}_{\text{adof}}\}\omega_e^2 \sin(\omega_e t) \tag{2}$$

where $\mathbf{M}$ is the mass matrix, $\mathbf{C}$ is the damping matrix, $\mathbf{K}$ is the stiffness matrix, $\mathbf{Y}$ is the generalised displacement vector for both beams, $\mathbf{Y}_{\text{adof}}$ is a vector with unit entries corresponding to the translational degrees of freedom for the base excitation, $\mathbf{F}_{\text{imp}}$ is the impact force vector having non-zero entries with opposite sign corresponding to the degrees of freedom where the impact occurs, α is the base excitation amplitude and ω_e is the base excitation frequency.

The magnitude of base excitation and the coupling spring constant were fixed at 0.2 mm and 10^3 N/m respectively. Time integration was performed using the fourth-order Runge–Kutta method with a variable time step. Proportional modal damping was included in the coupled system beams and the damping coefficient (ζ) was assumed to be 0.5%. Model reduction was applied to the system and the system was projected to a reduced modal space. Modal reduction cuts off the energy from the higher modes which has higher damping hence will not have significant influence on the beam response. The duration of penetration or contact is shown in Fig. 2 and the bandwidth excited is inversely proportional to the contact duration [30]. This spans approximately the first 12 modes of the individual beams. The next stage is to determine the parametric dependence of the system.

2.1. Parametric study on the beam response bandwidth

A parametric study was carried out using a sine sweep across a frequency range for two different clearances between the beams. The magnitude of base excitation and the coupling spring constant were fixed at 0.2 mm and 10^3 N/m respectively. The system was analysed for two different clearances of 5 mm and 90 mm between the beams. A sine sweep in frequency was carried out from 0 to 35 Hz with a step size of 0.5 Hz for each of the clearance cases. The maximum amplitude from the temporal response corresponding to each excitation frequency was determined. Fig. 3 shows the variation in the response for two different clearances between the beams. It can be observed that for a clearance of 5 mm the response of the system at the resonance peaks are less sharp. For a low clearance the system response is non-linear with the non-linearity induced by the contact. However for the 90 mm clearance the resonance peaks become more distinct and typical of a linear system behaviour. For a high

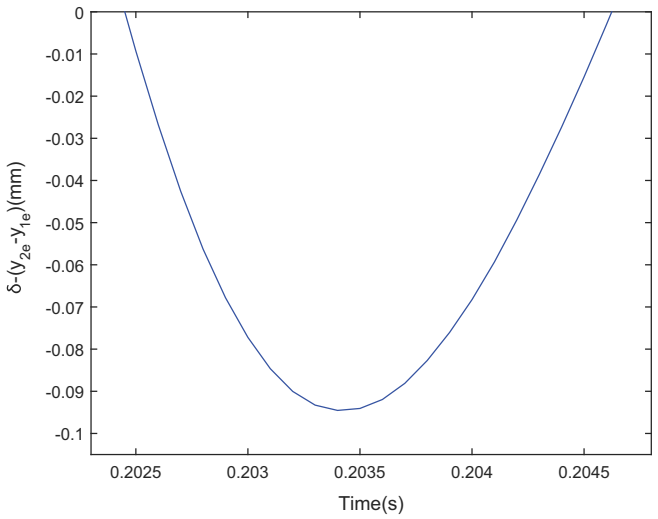

Fig. 2. Impact force duration.

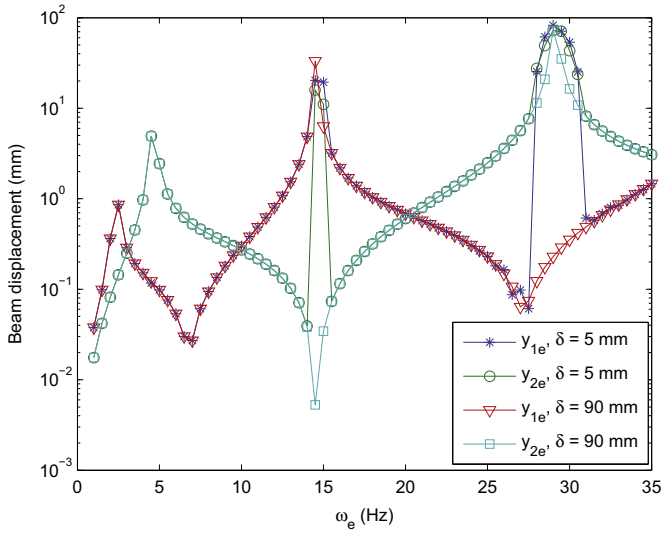

Fig. 3. The stepped sine responses of the thin beam (y_{1e}) and the thick beam (y_{2e}) for clearances of 5 and 90 mm, respectively, between the beams.

clearance between the two beams the response is linear, as expected. The system response for 5 mm clearance has an increase in response near 14 Hz and 30 Hz, which are close to the second natural frequencies of the thin and thick beams respectively.

Since the response of the system was relatively high at 29.09 Hz further analysis was carried out by base exciting the system at this frequency. The temporal variation in the clearance between the beams is shown in Fig. 4(a). A negative value, i.e. $\delta < (y_{2e} - y_{1e})$, indicates that the beams are in contact. Fig. 4 (b) shows the spectrum of the contact force. The spectrum is generated by carrying out block averaging of the Fourier transform of the response from 40 to 100 s using 146 sections. The block averaging was carried out to smooth the response spectrum. The response is noisy due to the fact that the system contains both the steady and transient responses. The contact can be considered as repeated impacts with an impulse hammer which reduces the coherence of the response.

The advantage of using an energy harvester with non-linear impact is that the higher modes are excited and this feature is explored by exciting the system at 29.09 Hz. The response of the thick beam (y_{e2}) at the location of impact is analysed. The variation in the frequency response of the beam due to parametric variation in the excitation force and clearance between the beams was analysed. The block averaged response spectra of the system obtained corresponding to two different clearances of 5 and 20 mm between the beams are shown in Fig. 5(a). For the higher clearance case the response is linear with the peak amplitude occurring at the resonance of the thick beam. However for the system with reduced clearance it can be observed that more modes are excited in the response spectrum. A similar observation can be made with the variation in base excitation amplitude. Fig. 5(b) shows the block averaged frequency response function for a fixed clearance (δ) of 10 mm and two different base excitation amplitudes of 0.1 mm and 0.2 mm. For the lower base excitation amplitude the response of the system is linear with a single peak near the natural frequency of the thick beam however for the higher base excitation amplitude multiple peaks can be observed in the frequency spectrum corresponding to higher frequencies.

3. Piezoelectric modelling

The influence of system parameters on the beam responses was determined in the previous section. The beam responses determine the power generated and the next step is to analyse the effectiveness of the power generated from the piezoelectric patch. Piezoelectric material can be added to the beam in either unimorph or bimorph configuration [31–33]. For the present system a unimorph is considered and the details of the piezoelectric patch used are given in Table 3. The piezoelectric patch is attached to the root of the clamped beams as shown in Fig. 1. This position was chosen because a high curvature is expected at the root compared to other locations on the beam.

The mechanical deformation generates a voltage across the piezoelectric patch. This is the direct piezoelectric effect. The electrical voltage generates a feedback on the mechanical domain creating a moment proportional to the voltage.

The charge produced is proportional to the strain in the PZT which is proportional to y_2'' where y_2 is the deformation of the beam. The piezoelectric patch behaves electrically like a capacitor and the charge produced is assumed proportional to the slope of the modes at the nodes of the piezoelectric patch [32,31].

The mechanical domain equation of motion including converse piezoelectric effect is

$$\mathbf{M}\ddot{\mathbf{Y}} + \mathbf{C}\dot{\mathbf{Y}} + \mathbf{K}\mathbf{Y} + \mathbf{F}_{\text{imp}} - \boldsymbol{\theta}V = \alpha \mathbf{M}\mathbf{Y}_{\text{adof}}\omega_e^2 \sin(\omega_e t) \tag{3}$$

where $\boldsymbol{\theta}$ is a vector in the physical domain with entries at the rotational degrees of freedom in the reduced modal domain for the nodes corresponding to the extreme ends of the piezoelectric patch. The piezoelectric equation of motion including the direct piezoelectric effect is

$$C_p\dot{V} + \frac{V}{R} + \boldsymbol{\theta}^T\dot{\mathbf{Y}} = 0 \tag{4}$$

where C_p is the piezoelectric patch capacitance, V is the voltage, R is the load resistance and $\boldsymbol{\theta}^T\dot{\mathbf{Y}}$ incorporates the influence of mechanical displacement on the current generated from the piezoelectric patch. The average power scavenged between time t_1 and t_2 is calculated by integrating the temporal response as

$$P_{\text{avg}} = \frac{1}{T_2 - T_1}\int_{T_1}^{T_2} \frac{V(t)^2}{R} dt \tag{5}$$

3.1. Optimal resistance

For the present system the capacitance within the circuit is from the piezoelectric patch. The load resistance of the system can be varied in order to maximize the power generated. Liao et al.

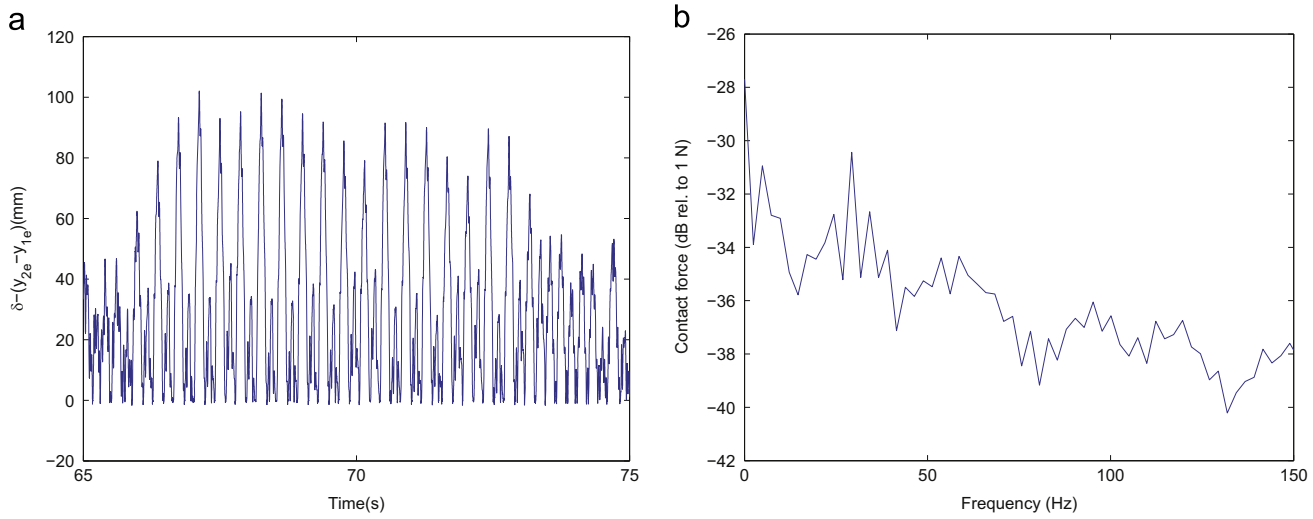

Fig. 4. Variation in the displacement of beams and the force spectrum for base excitation at 29.09 Hz. (a) Variation in clearance between the beams. (b) Impact force spectrum.

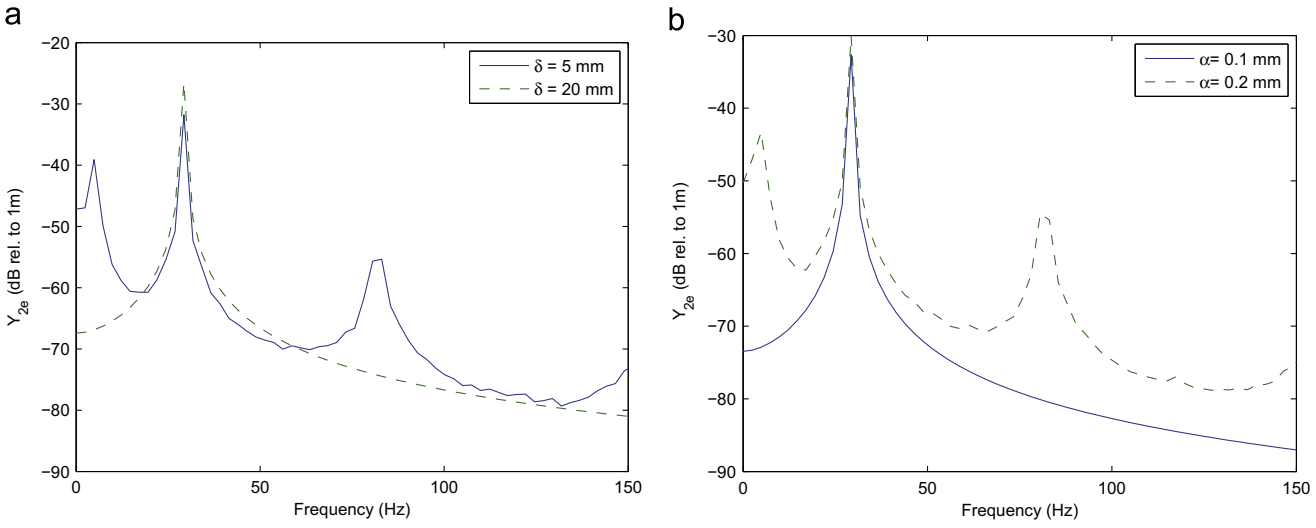

Fig. 5. Frequency responses variation with system parameters for a base excitation of the system at 29.09 Hz. (a) Frequency response for two different clearances between the coupled beams for a fixed base excitation amplitude α of 0.2 mm. (b) Frequency responses for two different base excitation amplitudes for a fixed clearance δ of 10 mm.

Table 3
Parameters of the Piezopatch.

Parameter	Value	Unit
Length of the piezo	28	mm
Thickness of the piezo	0.25	mm
Width of piezo	7	mm
Capacitance, C_p	51.4	nF
Resistance, R	0.2	MΩ
γ_c	4×10^{-5}	Nm/V

[34] analysed an RC circuit to determine the optimal system parameters to maximize the energy harvested. If the electromechanical coupling is weak, it was observed that the optimal resistance is approximately equal to $1/\omega C_p$ and for a higher coupling stiffness a correction term is required. The optimal resistance in our system using this approximate expression is 0.106 MΩ. The variation in the power generated with variation in the load resistance around the optimal value is shown in Fig. 6 and indicates that the approximate expression gives a good estimate of the optimal load resistance.

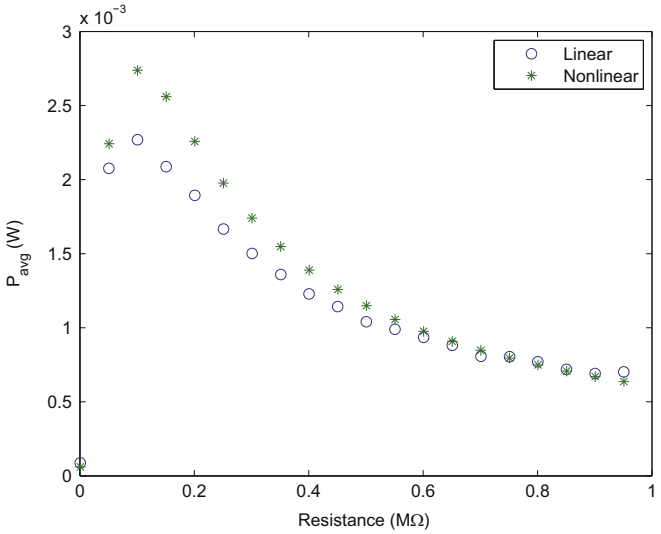

Fig. 6. Variation in the average power generated for various load resistance values.

3.2. Parametric study on power generation

A parametric study on different system parameters, namely the contact stiffness, damping and the clearance, was carried out, and the power generated was analysed. The load resistance was chosen as 0.1 MΩ. A frequency sweep was carried out from 0 to 35 Hz. The average power generated was estimated for each case and the results are plotted in Fig. 7. It can be observed from all the plots that the power is significantly higher at the resonance frequencies of the individual beams. Fig. 7(a) shows the variation in the average power generated across the frequencies for different contact stiffnesses. The contact causes higher frequencies to be excited, however contact can be considered as a constraint therefore increasing the contact stiffness could also restrict the beam responses. The constraint effect is dependent on the stiffness of the beam relative to the contact spring. Therefore the contact stiffness increase need not always result in an increase in power since it is an interplay between counteracting phenomena of broadband excitation and the constraint effect. The excitation of higher frequencies increases the power harvested however the constraint effects counteract it.

Fig. 7(b) shows the variation in the average power generated across the frequencies corresponding to different damping ratios, and it can be observed that with an increase in mechanical damping the spread across the peaks reduces which implies that the effectiveness of the harvester diminishes. However there is a caveat that in the physical system the converse piezoelectric effect also induces an influence on the beam responses similar to damping.

The influence of clearance on the power generated is shown in Fig. 7(c). It can be observed that with the reduced clearance the possibility of impact between the beams increases even in the frequency regions slightly away from the resonant peaks, where response amplitudes are generally lower.

3.3. Asymmetry and influence on power generation

The study until now has focussed on a fixed thickness ratio (z) between the beams. The influence of asymmetry on the system response can be analysed by varying the thickness ratio of the beams. The thicknesses of the beams influence the modal density within the bandwidth of excitation. The variation in the natural frequency of the uncoupled system for a fixed thickness of the thick beam and different thickness of the thin beam is shown in Fig. 8.

In order to understand the advantage of using a non-linear system a comparison with the power generated using a linear system was carried out. The single beam system was a base excited unimorph configuration. The beam was excited at $\omega_e = 29.09$ Hz

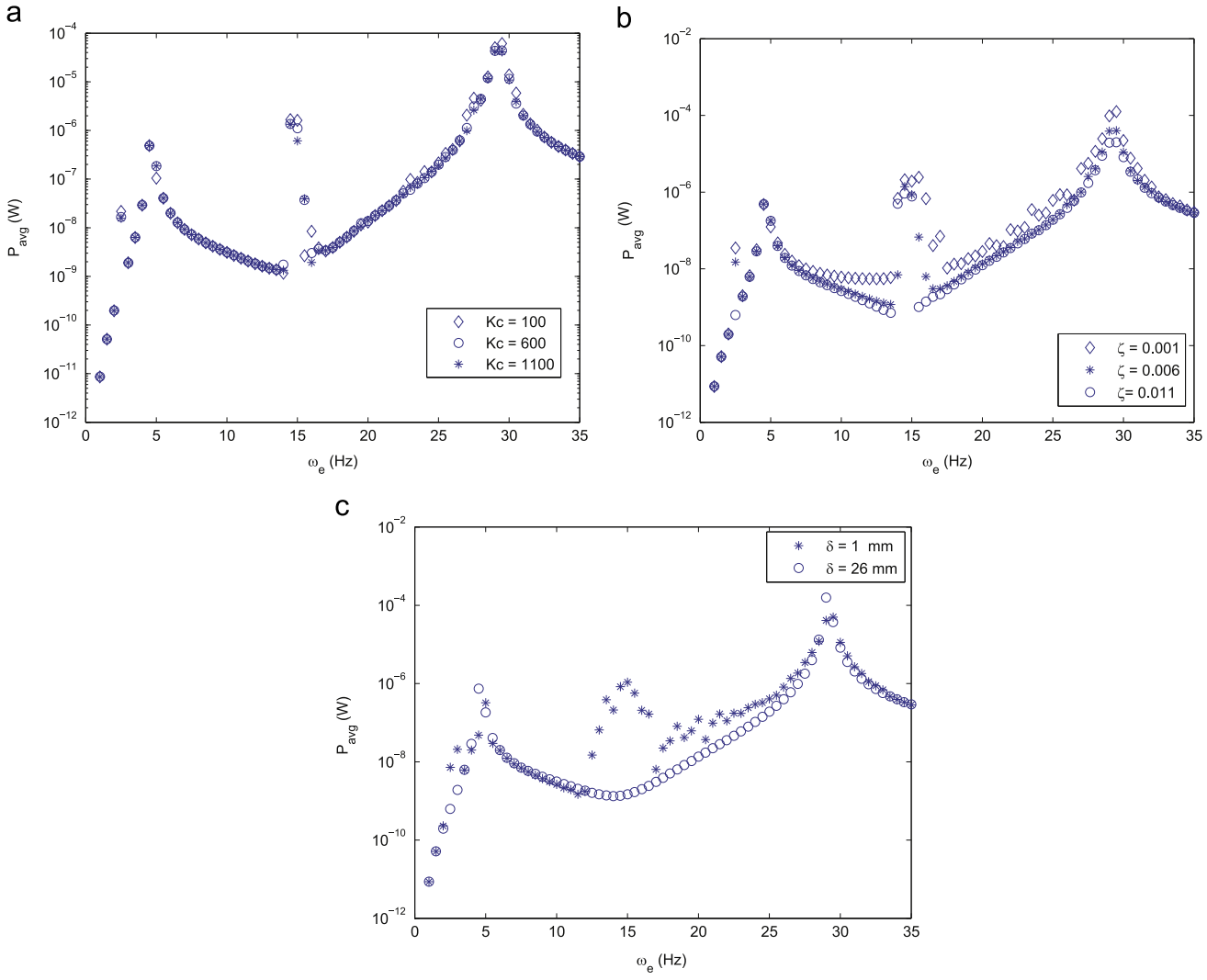

Fig. 7. Parametric study on the variation of power generated for a range of excitation frequencies and system parameters. (a) The effect of contact stiffnesses for a fixed $\zeta = 0.5\%$ and $\delta = 4$ mm. (b) The effect of damping ratio for a fixed $K_{cont} = 500$ N/m and $\delta = 4$ mm. (c) The effect of clearance for a fixed $K_{cont} = 500$ N/m and $\zeta = 0.5\%$.

which corresponds to the second natural frequency of the thick beam. The system was base excited with $\alpha = 0.2$ mm. The damping ratios of the beams were chosen as 1%. The thickness of the beam was varied and the variation in power generated is shown in Fig. 9(a). The peaks in the power generated are located at the thickness which produces a natural frequency at the excitation frequency of 29.09 Hz.

A similar study was carried out for the coupled beam system. The thickness of one beam was fixed at 0.5 mm and the thickness of the second beam was varied. Piezoelectric patches were attached to both beams in a unimorph series configuration. For the parametric study the general interest are in the thickness ratios where the thin and the thick beams have close modes. For these cases the interaction of the beam is very sensitive to the phase of the beam response. The power generated was analysed for two different clearances, 5 and 20 mm, between the beams and the results are shown in Fig. 9(b). For 20 mm clearance the response is less influenced by the thickness ratio variation and is similar to a single beam shown in Fig. 9(a). The difference of the coupled and the single beam system is that in the coupled beam system the thick beam is always resonating. However for 5 mm clearance the power generated is different from the single beam response. Since the thickness ratio modifies the frequencies and their spacing this also provides an indication of the broadband nature of the response for 5 mm clearance. For 5 mm clearance where the system is non-linear for most of the thickness ratios two distinct features can be noticed that are different from the linear system, namely high power generation is observed at a thickness ratio of 0.17 and a drastic drop in power compared to the linear system is observed near to a thickness of 0.45 mm.

For the 20 mm clearance case the response is mostly linear with the power generated being nearly twice the linear system at the resonant frequencies. The power was highest for both 5 and 20 mm clearances at the thickness ratio of 0.17 and frequencies of thick and thin beam were close. An analysis was carried out selecting two thickness ratios 0.16 and 0.17 and the corresponding voltage spectrum is shown in Fig. 10. The voltage spectrum was analysed since this would include the effects of both the thick and thin beams in the response. The frequencies within the 100 Hz bandwidth are shown and higher modes were not analysed. For the 0.16 and 0.17 thickness ratio the response is non-linear irrespective of the thickness for 5 mm clearance. However with a clearance of 20 mm the system behaves linearly.

A comparison of the voltage spectrum corresponding to the thickness ratios of 0.16 and 0.17 with a clearance of 5 mm is shown in Fig. 11. The number of modes excited due to impact within the bandwidth of 100 Hz is similar for two thickness ratios, as observed from Table 4 and the voltage spectrum in Fig. 11(c). The main difference between the two thickness ratios is the closeness of the natural frequencies of the thick and the thin beams, in relation to the base excitation frequency, since the system is excited near the second natural frequency of the thick beam.

The uncoupled natural frequencies of the system corresponding to 0.16 and 0.17 thickness ratios are given in Table 4. It can be observed that the frequency of the thick and the thin beams are close near to 5 Hz and 29 Hz. Frequencies other than the resonant frequencies are observed since the transients are always present due to the non-linear impact. The excitation of higher modes is also shown in Fig. 10. Since the system is asymmetric the coincident frequencies will have different mode shapes. Further analysis is carried out for the frequency near 29 Hz since the higher frequencies produce more power. For the frequency near 29 Hz the fourth mode of the thin beam is near the second mode of the thick beam. Since the close frequencies have different mode shapes the influence of the impact on the power generation could

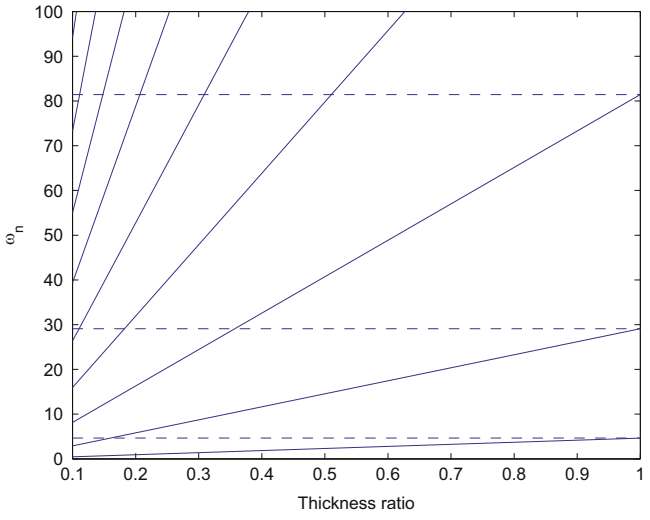

Fig. 8. Variation in natural frequency of thick and thin beams with thickness ratio. The horizontal dashed lines represent the natural frequencies of the thick beam, the thickness of which was fixed for the present study. The solid line represents the natural frequency of the thin beam.

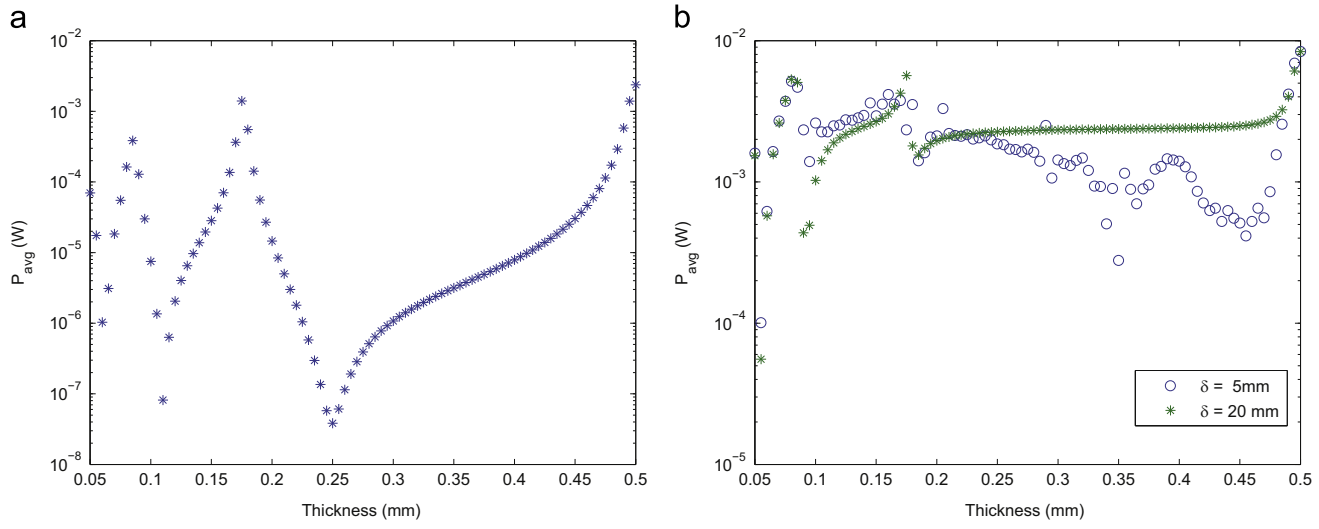

Fig. 9. Comparison of power generated using a single beam and coupled beam by exciting the system at $\omega_e = 29.09$ Hz. (a) Power generated from a single beam for different thicknesses. (b) Power generated in the coupled beam system for two different clearances by exciting the system at the second natural frequency.

be higher. A closer frequency match with respect to the excitation frequency is observed at the 0.17 thickness ratio resulting in higher power.

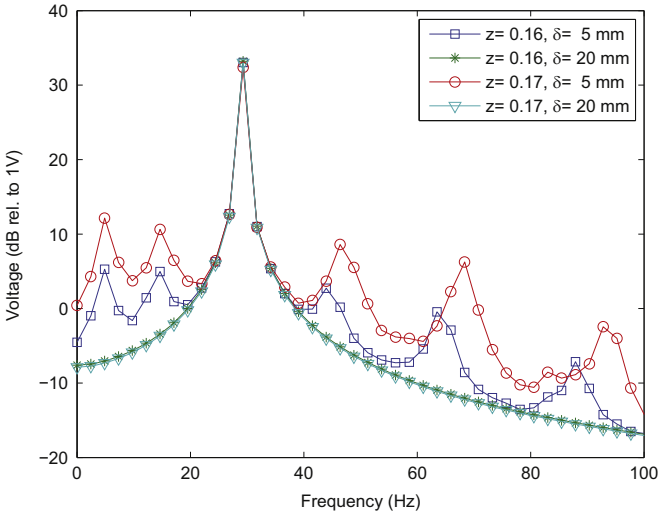

Fig. 10. Comparison of the voltage spectra for thickness ratios (z) of 0.16 and 0.17 for two different clearances between the beams.

In order to understand the reason for the higher power, the impact force spectrum was compared, as shown in Fig. 12. A higher impact force is generated for the thickness ratio of 0.17 which indicates a better interaction due to the non-linear impact.

A drop in power was observed when the thickness of the beams were nearly equal. A similar analysis was carried out for the thickness ratios of 0.79 and 0.91 which produced power of 4 and 1 μW respectively. The clearance between the beams was fixed at 5 mm. The natural frequencies of the system are shown in Table 5. As expected, since the dimensions are nearly the same, the frequencies and mode shapes should be similar. A comparison of

Table 4
Natural frequencies of the individual beams with thickness ratios of 0.16, 0.17 and 1.

Thickness ratio (z)		
0.16 ω_{thin}(Hz)	0.17 ω_{thin}(Hz)	1 ω_{thick}(Hz)
0.74	0.79	
4.65	4.94	4.64
13.03	13.84	
25.53	27.13	29.09
42.21	44.85	
63.06	67	

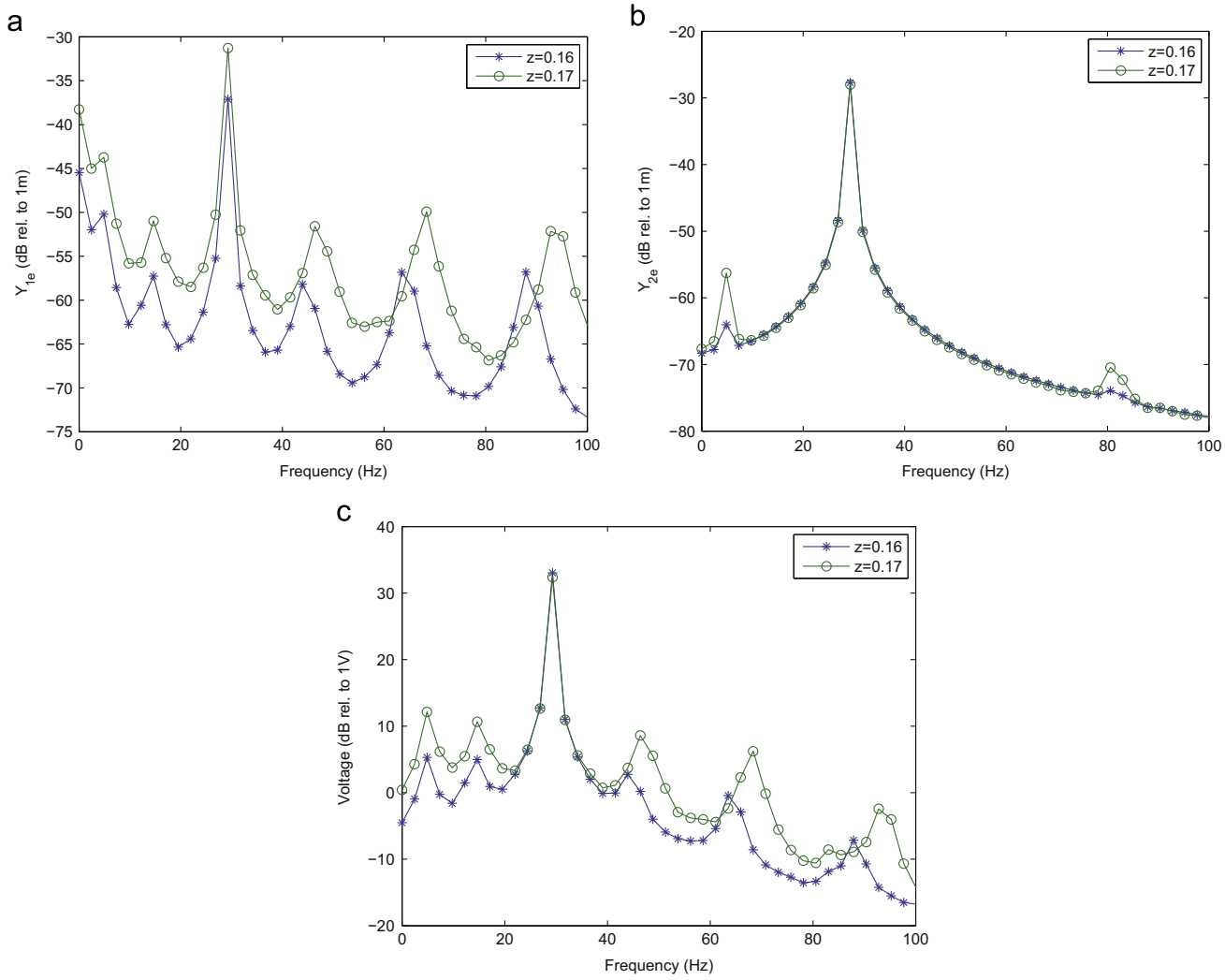

Fig. 11. Comparison of the displacement response and voltage spectra for thickness ratios of 0.16 and 0.17 with a clearance of 5 mm between the beams. (a) The thin beam response spectra. (b) The thick beam response spectra. (c) The voltage spectrum.

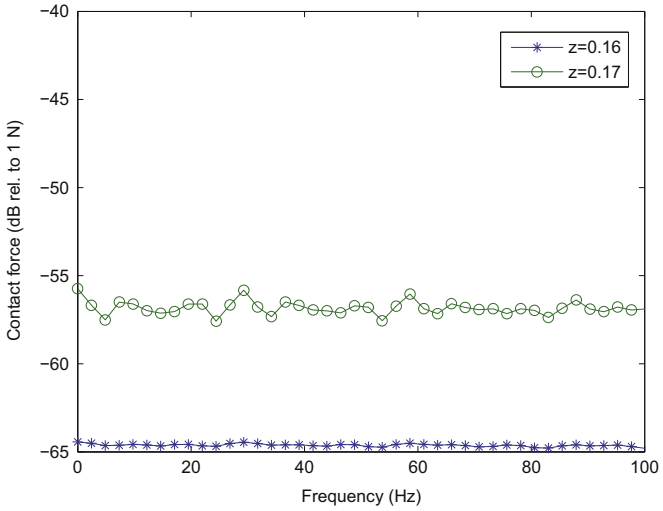

Fig. 12. Comparison of the contact force spectra for thickness ratios of 0.16 and 0.17 with 5 mm clearance between the beams.

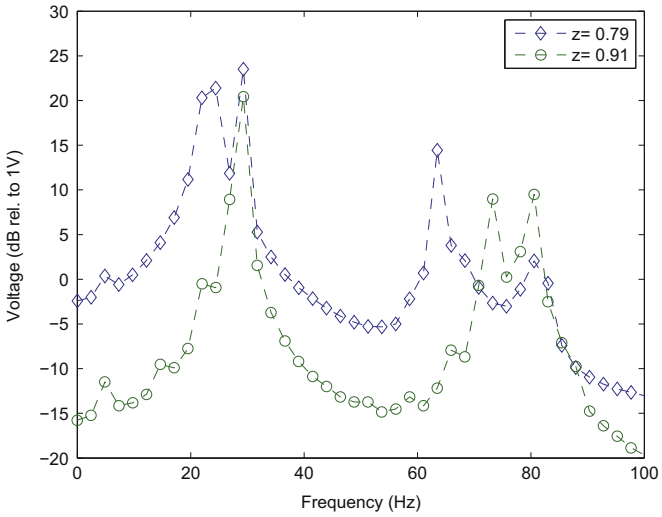

Fig. 13. Comparison of the voltage spectra for thickness ratios of 0.79 and 0.91 with 5 mm clearance between the beams.

Table 5
Natural frequencies of the individual beams with a thickness ratios (z) of 0.79, 0.91 and 1.

Thickness ratio (z)		
0.79 ω_{thin}(Hz)	0.91 ω_{thin}(Hz)	1 ω_{thick}(Hz)
3.67	4.2	4.64
22.98	26.5	29.09
64.34	74.1	81.44

the voltage spectrum is shown in Fig. 13. The number of modes excited is similar however the magnitudes are different, which could be due the fact that the modes are nearly in-phase and detuning of the system natural frequency by altering the thickness ratio modifies the power generated.

The results from the study indicate that the interacting modes within the bandwidth of excitation from impact influences the power generated from the harvester. A nearly symmetric structure which produces a high number of close modes does not necessarily produce high power since the interacting modes are nearly in phase thereby reducing the intensity of the impact.

4. Optimization study on controllable system parameters

The parametric study revealed that the controllable parameters such as the thickness, clearance and resistance can influence the power generated. The system can be optimised for these parameters with the objective of maximizing the power generated. A hypercube space with different thickness, clearance and resistance was spanned with 500 design points using Latin Hypercube Sampling (LHS) [35,36]. A nominal value of 0.3, 0.3 MΩ and 2.5 mm were chosen for the thickness ratio, resistance and clearance respectively. The design points were bounded within 0.1–2 $\times$ the nominal values. The standard deviation was chosen as 0.25 $\times$ the nominal value. A gradient based optimization [37–39] was carried out corresponding to each design point. An optimal power of 6 mW was obtained corresponding to thickness ratio of 0.168 was obtained corresponding to a resistance of 0.147 MΩ. The thickness ratio is near the maximum obtained from the parametric study and the resistance value was near the optimal. However the variation in power generated indicated less sensitivity to clearance within the optimization range.

5. Conclusion and discussion

The results from the study indicate that energy harvesting using impact is a viable option to improve the operational bandwidth of the harvester. Contrary to the linear system where only one mode is excited, with the non-linear impact more modes are excited for the same base excitation frequency. The key mechanical parameters of the system which can be used to control the performance are the clearance and the contact stiffness. Variation in contact stiffness alters the power depending, for a given thickness ratio and clearance, on whether the constraint effect (which reduces the power) or the broadband excitation (which increases the power) dominates the response.

The power generated is highly sensitive to the clearance and the thickness ratio. A higher clearance reduces the possibility of impact. The spectrum of the voltage generated with impact from the coupled system indicated multiple peaks due to the excitation of higher modes. The power generated depends on the number of close modes within the bandwidth excitation of non-linear impact. However it was observed that the close modes should have dissimilar mode shapes. For example the beams of similar dimensions will have all the uncoupled modes close by but will produce less power. This occurs because the mode shapes will be nearly identical, and hence it oscillates nearly in phase causing the constraint effect to dominate over the advantage gained from exciting the higher modes of the system. The results from the study indicate that by carefully detuning the frequencies and the contact stiffness of the system vibro-impact can produce more power than a linear system. The present optimization study indicates that the tuning of the thickness ratio is more crucial than clearance within the optimization range considered. The optimised parameters can be considered for further experimental validations. However the optimization carried out did not consider the length of the piezoelectric patch, as a continuous piezoelectric patch can cause cancellation of electric charges [40]. Since the multiple modes are excited further improvement in the power generated could be carried out using segmented piezoelectric patches [40,41].

Acknowledgements

The authors acknowledge the support of the Engineering and Physical Sciences Research Council through Grant no. EP/K003836 ("Engineering Nonlinearity").

References

[1] Vijayan K. Vibration and shock amplification of drilling tools [Ph.D. thesis]. University of Cambridge; 2012.
[2] Jiang Y, Masaoka S, Fujita T, Uehara M, Toyonaga T, Fujii K, et al. Fabrication of a vibration-driven electromagnetic energy harvester with integrated NdFeB/Ta multilayered micro-magnets. J Micromech Microeng 2011;21(9).
[3] Khan F, Sassani F, Stoeber B. Copper foil-type vibration-based electromagnetic energy harvester. J Micromech Microeng 2010;20(12):125006.
[4] Tvedt LGW, Nguyen DS, Halvorsen E. Nonlinear behavior of an electrostatic energy harvester under wide- and narrowband excitation. J Microelectromech Syst 2010;19:305–16.
[5] Anton Steven R, Sodano Henry A. A review of power harvesting using piezoelectric materials (2003–2006). Smart Mater Struct 2007;16:R1–21.
[6] Beeby SP, Tudor MJ, M White N. Energy harvesting vibration sources for microsystems applications. Meas Sci Technol 2006;17(12):175–95.
[7] Roundy S, Wright PK, Rabaey J. A study of low level vibrations as a power source for wireless sensor nodes. Comput Commun 2003;26:1131–44.
[8] Paci D, Schipani M, Bottarel V, Miatton D. Optimization of a piezoelectric energy harvester for environmental broadband vibrations. In: Fifteenth IEEE international conference on electronics, circuits and systems, 2008. ICECS 2008; 2008. p. 177–81.
[9] Miller LM, Halvorsen E, Dong T, Wright PK. Modelling and experimental verification of low frequency MEMS energy harvesting from ambient vibrations. J Micromech Microeng 2011;21:045029.
[10] Jiang S, Li X, Guo S, Hu Y, Yang J, Jiang Q. Performance of a piezoelectric bimorph for scavenging vibration energy. Smart Mater Struct 2005;14(4):769.
[11] Shunong Jiang, Hu Yuantai. Analysis of a piezoelectric bimorph plate with a central-attached mass as an energy harvester. IEEE Trans Ultrason Ferroelectr Freq Control 2007;54(7):1463–9.
[12] Hu HP, Cui ZJ, Cao JG. Performance of a piezoelectric bimorph harvester with variable width. J Mech 2007;23(03):197–202.
[13] Hu Y, Xue H, Hu H. A piezoelectric power harvester with adjustable frequency through axial preloads. Smart Mater Struct 2007;16(5):1961.
[14] DuToit NE, Wardle BL, Kim SG. Design considerations for mems-scale piezoelectric mechanical vibration energy harvesters. Integr Ferroelectr 2005;71(1):121–60.
[15] Daqaq MF. Response of uni-modal Duffing-type harvesters to random forced excitations. J Sound Vib 2010;329(18):3621–31.
[16] Mann BP, Sims ND. Energy harvesting from the nonlinear oscillations of magnetic levitation. J Sound Vib 2009;319:515–30.
[17] Sebald G, Kuwano H, Guyomar D, Ducharne B. Experimental duffing oscillator for broadband piezoelectric energy harvesting. Smart Mater Struct 2011;20.
[18] Nguyen DS, Halvorsen E, Jensen GU, Vogl A. Fabrication and characterization of a wideband MEMS energy harvester utilizing nonlinear springs. J Micromech Microeng 2010;20(12):125009.
[19] Umeda M, Nakamura K, Ueha S. Analysis of transformation of mechanical impact energy to electrical energy using a piezoelectric vibrator. Jpn J Appl Phys 1996;35(Part 1, No. 5B).
[20] Gu L, Livermore C. Impact-driven, frequency up-converting coupled vibration energy harvesting device for low frequency operation. Smart Mater Struct 2011;20(4):045004.
[21] Jacquelin E, Adhikari S, Friswell MI. A piezoelectric device for impact energy harvesting. Smart Mater Struct 2011;20(10).
[22] Soliman MSM, Abdel-Rahman EM, El-Saadany EF, Mansour RR. A wideband vibration-based energy harvester. J Micromech Microeng 2008;18:115021.
[23] Rastegar J, Murray R, Pereira C, Nguyen HL. Novel piezoelectric-based energy-harvesting power sources for gun-fired munitions, SPIE 14th Annual international symposium on: smart structures and materials & nondestructive evaluation and health monitoring. International Society for Optics and Photonics; 2007, 6527-32.
[24] Harne RL, Wang KW. A review of the recent research on vibration energy harvesting via bistable systems. Smart Mater Struct 2012;22:023001.
[25] Babitsky VI. Theory of vibro-impact systems and applications. Berlin, Heidelberg: Springer-Verlag; 1998.
[26] Yang Zengtao, Yang Jiashi. Connected vibrating piezoelectric bimorph beams as a wide-band piezoelectric power harvester. J Intel Mater Syst Struct 2009;20:569–74.
[27] Petropoulos T, Yeatman EM, Mitcheson PD. MEMS coupled resonators for power generation and sensing. Micromechanics Europe, Leuven, Belgium; 2004.
[28] Vijayan K, Woodhouse J. Shock transmission in a coupled beam system. J Sound Vib 2013;332:3681–95.
[29] Vijayan K, Woodhouse J. Shock amplification, curve veering and the role of damping. J Sound Vib 2014;333(5):1379–89.
[30] Inman DJ, Singh RC. Engineering vibration, vol. 3. Upper Saddle River: Prentice-Hall; 2001.
[31] Friswell MI, Ali SF, Bilgen O, Adhikari S, Lees AW, Litak G. Nonlinear piezoelectric vibration energy harvesting from a vertical cantilever beam with tip mass. J Intel Mater Syst Struct 2012;23(13):1505–21.
[32] Erturk A, J Inman D. Piezoelectric energy harvesting. Chichester, UK: Wiley; 2011.
[33] Priya S, Inman DJ, editors. Energy harvesting technologies. Springer US; 2009.
[34] Liao Y, Sodano HA. Optimal parameters and power characteristics of piezoelectric energy harvesters with an rc circuit. Smart Mater Struct 2009;18(4):045011.
[35] McKay MD, Beckman RJ, Conover WJ. A comparison of three methods for selecting values of input variables in the analysis of output from a computer code. Technometrics 2000;42(1):55–61.
[36] Iman RL. Latin hypercube sampling. New York: Wiley Online Library; 2008.
[37] Antoniou A, Lu WS. Practical optimization: algorithms and engineering applications. Springer US; 2007.
[38] Christensen Peter W, Klarbring Anders. An introduction to structural optimization. Springer Netherlands; 2009.
[39] Cavazzuti Marco. Optimization methods: from theory to design scientific and technological aspects in mechanics. Springer-Verlag Berlin Heidelberg; 2013.
[40] Erturk A, Tarazaga PA, Farmer JR, Inman DJ. Effect of strain nodes and electrode configuration on piezoelectric energy harvesting from cantilevered beams. J Vib Acoust 2009;131(1):011010.
[41] Friswell MI. On the design of modal actuators and sensors. J Sound Vib 2001;241(3):361–72.